


Effect of interfacial modification on functional properties of polyethylene and polypropylene—Fibrous silica nanocomposites

Aziz Fihri¹  | Jevgenij Lazko² | Fouad Laoutid² | Jérôme Mariage² | Julie Passion² | Tim Schow² | Yassine Malajati¹ | Ruchi Rastogi¹ | Haleema Alamri¹ | Philippe Dubois²

¹Non-Metallic Application Development Division, Research & Development Center, Saudi Aramco, Dhahran, Kingdom of Saudi Arabia

²Laboratory of Polymeric and Composite Materials, Materia Nova Research Center, Mons, Belgium

Correspondence

Aziz Fihri, Non-Metallic Application Development Division, Research & Development Center, Saudi Aramco, Dhahran 31311, Kingdom of Saudi Arabia.

Email: aziz.fihri@aramco.com

Abstract

This paper reports the results of polyethylene (PE) and polypropylene (PP) composites containing 5 and 10 wt.% dendritic fibrous nanosilica (DFNS) synthesized by a hydrothermal process. The objective of this investigation is to provide a better understanding of the relationship between the structure, composition, matrix-nanofiller interfaces, and the properties of these nanocomposites. These materials have been prepared by twin-screw extrusion and injection molding. Their structural, thermal, mechanical, rheological, and electrical properties were evaluated, both alone and when combined with an organic compatibilizing agent. Findings have shown that the unique morphology of fibrous silica nanoparticles was preserved and not altered by melt processing, indicating the high thermal and mechanical stability of these fibrous materials. The nanocomposites containing DFNS alone exhibited higher mechanical performances compared to those containing the surface modifier, with no observable effect on their thermal properties. Findings also showed that the interactions between the nanoparticles and polymer may influence the functional properties of the final nanocomposites, and that they are dependent on both the nature of the host polymer along with the presence of the surface modifier agent.

Highlights

- Well-defined DFNS were successfully prepared.
- PE and PP based nanocomposites were successfully designed by twin-screw extrusion.
- Good interfacial interactions were obtained with PP.
- Functional properties of the nanocomposites were influenced by the interfacial adhesion.

KEYWORDS

composites; dendritic fibrous nanosilica; functional properties; melt processing; interface; polyethylene; polypropylene; reinforcement agent

1 | INTRODUCTION

Polyolefins such as polyethylene (PE) are cost-effective polymers, with good processability and a wide range of properties and applications. Polyolefin-based nanocomposites have been widely studied for developing strong and multifunctional materials, with enhanced mechanical, thermal, flame-retardant, and gas-barrier properties.¹ The development of high-performance nanocomposites requires uniform and homogeneous distribution and dispersion of nanoparticles as well as good interfacial adhesion with the host polymeric matrix, regardless of their chemical structure and shape. This is often achieved by (i) using compatibilizing compounds, or (ii) by chemical modification of the surface of the nanoparticles, using designed molecules that present good affinity with the polymer for strengthening the filler matrix interface.^{2,3} The compatibility of non-polar polymers, such as PE and polypropylene (PP), with polar fillers such as metallic oxide nanoparticles, is often achieved through the incorporation of compatibilizers such as PE or PP grafted with polar functions such as maleic anhydride for example⁴⁻⁶ or by using nanosilica surface-modified by organosilane coupling agents.^{7,8} However, the search for alternative processes for improving the adhesion between polymers and nanofillers, and thus avoiding time consuming nanoparticles surface modification and compatibilizer preparation, is still an active area of research. Recently, Russo et al.⁹ demonstrated that nanoparticle architectures play a major role in the physical interaction at the polymer-filler interface. Using “wrinkled” silica nanoparticles into polylactide favored more effective particle-particle interactions, due to the greater physical interaction with the surrounding polymeric matrix, than when smooth silica nanoparticles are used. Other studies demonstrated that the diffusion of the polymeric chains into nanometric-sized pores of mesoporous silica particles, used as reinforcement nanofillers, enhanced the interfacial interactions and strongly suppressed nanoparticles' aggregation.^{10,11} Dendritic fibrous nanosilica (DFNS) has attracted great interest thanks to its unique properties such as the open pore structure compared to numerous popular silica materials.¹² The exact mechanism of the formation of the dendritic silica structure is still unclear and under scientific debate.¹³ DFNS was tested for a range of applications including catalysis, CO₂ capture, and corrosion where good activities were observed.^{14,15} To our best of knowledge, the use of this new class of fibrous silica as a ¹reinforcement agent for polyolefins has not been explored to this day.

In the present work, we have investigated the effect of incorporating fibrous silica nanoparticles both alone

and in combination of organic surface modifier, on the thermal, morphological, mechanical, rheological, and electrical properties of PE and PP nanocomposites. Towards this goal, PE and PP based nanocomposites containing 5 and 10 wt.% DFNS, alone and in combination with 1 wt.% K-STOFF (a fatty acid derivative) were produced using twin screw extrusion and injection molding. The performance of the developed composites was tested and the results are reported in the current work.

2 | EXPERIMENTAL SECTION

2.1 | Materials

Tetraethyl orthosilicate (TEOS, 98%), hexadecyltrimethylammonium bromide (CTAB, >99%), urea (>98%), toluene (99.7%), and 1-pentanol (>99%) reagents were purchased from by the Sigma-Aldrich chemical company and used without further purification. Cyclohexane (>99%) was purchased from Fisher scientific. High-density PE (DOW KT 10000) from DOW and PP PCH26 from SABIC were purchased from Resinex (Belgium). K Stoff T(KST) additive based on fatty acid and amide derivatives (20 Microns Nano Minerals Limited, India) was provided by Xatico (Belgium).

2.2 | Fibrous silica nanoparticles synthesis

DFNS particles were synthesized via a hydrothermal process as reported previously.^{15,16} Briefly, TEOS (25 g), cyclohexane (310 mL), and 1-pentanol (16 mL) were mixed and left for stirring at room temperature for 30 minutes. Concurrently, an additional solution including CTAB (8 g), urea (6 g), and deionized water (310 mL) was also prepared and stirred at room temperature for 30 min. The TEOS solution was then added to the CTAB and urea solution and stirred for 1 h. The solution was then transferred into an autoclave and heated at 130°C for 5 h. The suspension was cooled down to ambient temperature and the powder was isolated by centrifugation, washed with water and ethanol then calcined at 550°C for 4 h. The mean diameters d₃₂ and d₄₃ of DFNS, determined by image analysis of electron microscopy pictures (Figure 1), were around 500 and 550 nm, respectively.

Upon SEM analysis, it was determined that the synthesized silica exhibited a fibrous structure spreading out in a radial manner and distributed in a flower-like behavior in all directions as depicted in Figure 1. FSN demonstrated high thermal stability as revealed by thermogravimetric analysis measurements (Figure 2) performed under inert

¹reinforcement agent

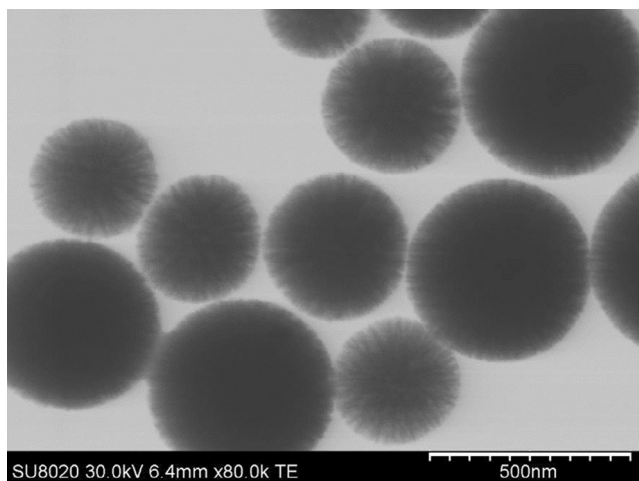


FIGURE 1 SEM images (TE mode) of synthesized dendritic fibrous nanosilica.

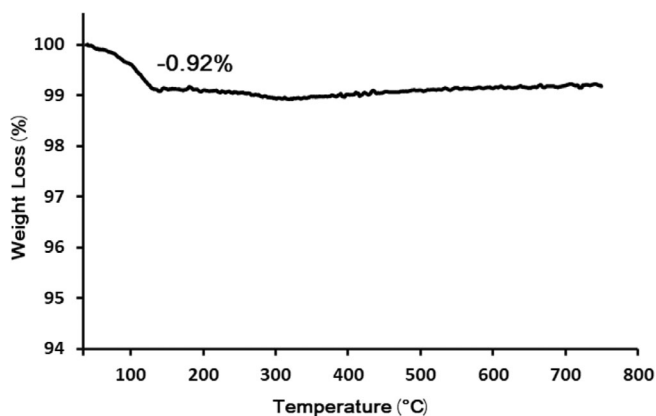


FIGURE 2 TGA curve of dendritic fibrous nanosilica particles.

atmosphere. Indeed, only an initial weight loss of 1% was observed around 100°C which could be attributed to the evaporation of physisorbed water and confirms that the surfactant was completely removed during the calcination process.

2.3 | Composite preparation by melt processing

PE and PP-DFNS nanocomposites were prepared by extrusion using Thermo Scientific Process 11 twin screw extruder (Thermo Fisher Scientific, USA) at 180 and 190°C, respectively. The investigated compositions are summarized in Table 1. The so-obtained PE-DFNS and PP-DFNS pellets were used for the preparation of specimens for mechanical testing and rheological analysis by injection molding using Haake Mini Jet Pro laboratory scale injection-molding equipment (Thermo Fisher Scientific, USA) at 180 and 190°C, respectively.

2.4 | Characterization

Differential scanning calorimetry (DSC) was carried out using Discovery DSC 25 (TA Instruments, USA), with standard 3 cycle heating-cooling-heating method, between 60 and 230°C, at 20°C/min. Thermal stability of DFNS was determined by thermal gravimetric analyses (TGA) with a TGA 2 (Mettler-Toledo GmbH, Greifensee, Switzerland) by heating the sample under nitrogen from room temperature to 800°C at 20°C/min. Scanning electron microscopy (SEM) analysis was performed using XL 20 Phillips field emission gun scanning electron microscope (FEG-SEM) (Hitachi High Technologies, Japan). SEM observations have been performed on fibrous silica nanoparticles, previously resuspended in ethanol, in transmission mode (TE), and on cryo-fractured PE and PP nanocomposites coated with gold, using the secondary electron mode (SE-U). Melt Flow Index (MFI) measures were carried out using Ray-Ran Melt flow indexer RR 3000 (Tinius Olsen, UK), under 2.16 kg mass at 190°C for PE and related nanocomposites and at 230°C for PP-based materials. Stress-strain tensile tests were carried out using Lloyd LR 10 K apparatus (Lloyd Instruments LTD, UK) equipped with 1000 N load cell, with standard 25.4 mm dog-bone specimens, at 20°C and 10 mm/min speed, according to ISO 527 and ASTM D638 standards. For each formulation at least 5 samples were tested to obtain Young's modulus, Yield stress, Yield strain, Stress at break, and Elongation at break values. Flexural characterizations were carried out according to ISO 178 (D790-03) 3 points method using Lloyd LR 10 K equipment (Lloyd Instruments LTD, UK) with 80 × 10 × 4 mm specimens, at 20°C and 2 mm/min speed. For each formulation at least five samples were tested to obtain flexural modulus and Strength. Impact tests were performed using Ray-Ran 2500 Advanced Pendulum Impact System (Ray-Ran Polytest, UK) with IZOD method according to ISO 180 and ASTM D256 standards. For each formulation, at least five 63.5 × 12.0 × 3.2 mm rectangular samples were tested to determine impact strength value and fracture type. Rheological measurements were carried out at 180°C, using Anton Paar Rheometer MCR 302, on PE, PP, and nanocomposites containing 10 wt.% DFNS, with and without K-STOFF T. Viscosity was measured in the dynamic regime in the shear rate range from 0.10 to 100 rad/s at 1% deformation.

3 | RESULTS AND DISCUSSION

The effect of incorporating DFNS particles on the functional properties of PE and PP nanocomposites was evaluated both with and without an amide derivative of fatty acid (K-STOFF) as a surface modifying agent. Results are presented in the following sections.

Reference	PE (wt.%)	PP (wt.%)	DFNS (wt.%)	K-Stoff (wt.%)
PE-0	100	/	0	0
PE-5	95	/	5	0
PE-10	90	/	10	0
PE-0-K	99	/	0	1
PE-5-K	94	/	5	1
PE-10-K	89	/	10	1
PP-0	/	100	0	0
PP-5	/	95	5	0
PP-10	/	90	10	0
PP-0-K	/	99	0	1
PP-5-K	/	94	5	1
PP-10-K	/	89	10	1

TABLE 1 Content of PE, PP, DFNS, and K-Stoff used for the preparation of polymer blends.

TABLE 2 Melt flow index of PE and PP nanocomposites.

Reference	MFI [g/10 min]
PE-0	7.7 ± 1.3
PE-5	7.2 ± 0.9
PE-10	6.2 ± 0.4
PE-0-K	8.1 ± 0.3
PE-5-K	7.0 ± 0.3
PE-10-K	6.7 ± 0.5
PP-0	9.3 ± 0.8
PP-5	9.3 ± 0.9
PP-10	8.2 ± 1.0
PP-0-K	10.2 ± 1.0
PP-5-K	9.7 ± 1.0
PP-10-K	9.1 ± 1.2

3.1 | Melt flow index

MFI test is a simple method, usually used in industry, to estimate the flow properties of polymers and composites at their melting state. This approach was also used in the present study. The effect of the incorporation of DFNS on the melt flow of PE and PP composites is presented in Table 2. The incorporation of nanoparticles such as organoclays may induce important viscosity increase, that can affect polymer chains mobility and nanocomposite melt processing, especially during the injection molding step of highly loaded samples.^{17,18} However, in the present case, the incorporation of fibrous silica nanoparticles did not induce any significant reduction of nanocomposite melt flow. MFI decrease was limited and remained around 7 g/10 min for the different PE-based compositions, and around 9 g/10 min for PP-based nanocomposites. Moreover, this behavior was not

changed by using the K-STOFF surface modifying agent since the MFI values remained very similar to those of binary nanocomposites without K-STOFF. This observation is in agreement with results reported in previous studies where similar behavior was observed for tertiary PP/silica formulations with stearic acid interfacial modifier.¹⁹

3.2 | Mechanical properties

Tensile and impact properties of PE and PP containing DFNS, with and without K-STOFF surface modifying agent, are presented in Table 3. In the case of binary PE composites, the incorporation of 5 wt.% DFNS did not significantly affect the material tensile properties. In fact, Young's modulus remains at around 1300 MPa. The stress and strain at yield are equal to 30 MPa and 7%, respectively while elongation at break remains higher than 300%. However, increasing DFNS content up to 10 wt.% caused an important reduction of the material's ductility because the elongation at break decreased down to 60% while Young's modulus remained unchanged (around 1300 MPa). Furthermore, the tensile properties of PP seemed to be more affected by the presence of DFNS, even at low incorporation rates (5 wt.%). In fact, the elongation at break decreases from 216 to 100% when 5 wt.% DFNS are incorporated, without affecting either Young's modulus or stress at yield. At high incorporation rate, that is, 10 wt.%, the presence of DFNS induced important reduction of the material ductility down to 50%. DFNS nanoparticles appear to be significantly influenced by the nature of the polymeric matrix. The effect of DFNS particles appear to be in a non-negligible way dependent on the nature of the polymeric matrix. Moreover, for tertiary formulations, the K-STOFF influence

TABLE 3 Tensile and impact properties of PE-DFNS and PP-DFNS nanocomposites.

Reference	Young's modulus (Mpa)	Stress at yield (MPa)	Strain at break (%)	Impact resistance (kJ/m ²)	Fracture type
PE-0	1300 ± 30	30.0 ± 0.7	390 ± 70	10.4 ± 1.0	Partial
PE-5	1360 ± 60	30.6 ± 0.4	315 ± 80	5.7 ± 0.2	Partial
PE-10	1360 ± 40	31.7 ± 0.4	60 ± 25	4.0 ± 0.3	Partial
PE-0-K	1246 ± 56	30.0 ± 0.6	350 ± 80	8.4 ± 0.4	Partial
PE-5-K	1494 ± 40	31.0 ± 0.7	100 ± 50	4.5 ± 0.2	Partial
PE-10-K	1431 ± 61	32.7 ± 2.7	25 ± 7	3.0 ± 0.2	Complete
PP-0	1380 ± 40	26.7 ± 0.9	216 ± 50	55 ± 5	Non break
PP-5	1340 ± 100	25.6 ± 0.5	106 ± 40	24 ± 2	Partial
PP-10	1320 ± 80	24.0 ± 0.4	50 ± 24	17 ± 3	Partial
PP-0-K	1144 ± 125	23.9 ± 2.0	291 ± 26	59 ± 2	Non break
PP-5-K	1243 ± 30	23.6 ± 0.5	130 ± 55	27 ± 10	Partial
PP-10-K	1183 ± 70	22.5 ± 1.0	29 ± 7	13 ± 1	Complete

was also more pronounced for PE than for PP composites, with surprisingly, considerably strong reduction of the elongation at break down to 25%. For PP-based tertiary blends, the presence of K-STOFF did not induce any significant change in the ductility of the material, with elongations at break mainly remaining around 120 and 40% at 5 and 10 wt.% filler contents, respectively.

Incorporation of DFNS particles had also resulted in reducing impact behavior. Moreover, in the presence of the surface modifier, the impact resistance of different nanocomposites was not enhanced, but even slightly reduced in some cases. In fact, the incorporation of 1 wt.% K-STOFF led to a reduction of the impact resistance of 10 wt.% PE-DFNS nanocomposite, from 4 to 3 kJ/m² and to a change of the failure mode, from partial to complete fracture (Table 3). Similar behavior was observed in the case of PP. Impact resistance decreased from 17 to 13 kJ/m² when 1 wt.% K-STOFF is combined with fibrous silica nanoparticles. The positive reinforcing effect of DFNS is however well pronounced on the flexural properties of PE and PP, since the incorporation of DFNS leads to a significant increase in flexural modulus from 780 up to 1020 MPa in the case of PE and from 1120 up to 1360 MPa in the case of PP (Table 4). Flexural strength is also enhanced from 17.0 to 21.7 MPa and from 27.6 to 29.7 MPa when 10 wt.% DFNS is incorporated into PE and PP, respectively.

However, the combination of DFNS and K-STOFF seems to counteract the reinforcing effect of DFNS alone. Association of these two additives does not lead to any change in the flexural modulus of PE-based nanocomposites but interestingly leads to a decrease in the flexural modulus of PP blends. Once again, the performances behavior of DFNS, when combined with the interfacial

TABLE 4 Flexural properties of PE-DFNS and PP-DFNS composites.

Reference	Flexural modulus (MPa)	Flexural strength (MPa)
PE-0	780 ± 50	17.0 ± 0.7
PE-5	940 ± 45	20.5 ± 0.1
PE-10	1020 ± 60	21.7 ± 0.4
PE-0-K	860 ± 50	18.8 ± 0.3
PE-5-K	1060 ± 100	19.5 ± 0.5
PE-10-K	1000 ± 60	21.4 ± 0.7
PP-0	1120 ± 60	27.6 ± 0.4
PP-5	1350 ± 35	30.2 ± 0.3
PP-10	1360 ± 22	29.7 ± 0.5
PP-0-K	1040 ± 40	22.8 ± 0.9
PP-5-K	1070 ± 30	24.6 ± 0.6
PP-10-K	1140 ± 40	26.4 ± 0.4

agent, depends on the nature of the host polymeric matrix.

The observed reduction in elongation at break, for nanocomposite containing 10 wt.% DFNS could be attributed to (i) an increase of the polymer crystallinity induced by the addition of the nanoparticles, (ii) poor interfacial adhesion between the matrix and nanoparticles, or (iii) due to the presence of large aggregates of nanoparticles. Any of these three reasons can lead to the formation of brittle zones, which can induce a premature material failure and explain the observed reduction in the impact resistance of PE and PP nanocomposites. In fact, the incorporation of relatively low K-STOFF content (1 wt.%) has been carried out

TABLE 5 DSC properties of pristine PE and PP polymers and related nanocomposites.

	Crystallization		Melting	
	T_c (°C)	ΔH_c (J/g)	T_m (°C)	ΔH_f (J/g)
PE-0	114	220	136	229
PE-5	113	197	140	204
PE-10	112	204	140	215
PE-0-K	112	210	140	211
PE-5-K	116	220	140	233
PE-10-K	115	206	138	215
PP-0	121	77	167	74
PP-5	127	80	168	77
PP-10	127	78	168	76
PP-0-K	118	77	166	73
PP-5-K	120	77	166	72
PP-10-K	120	76	166	72

in both unfilled polymers and nanocomposites with the specific aim to enhance the nanoparticles dispersion state and the interfacial adhesion between the polar silica surface and the non-polar PE and PP matrices. Indeed, K-STOFF is a fatty acid-amide derivative that is claimed to improve mechanical properties of composites through favoring better homogeneous dispersion of pigments, fillers, and additives within polyolefins.²⁰ Nevertheless, in the case of our study, the results obtained were different from what was expected. Further investigations were carried out to understand the origin of changes in the mechanical properties obtained with DFNS in the presence and absence of the surface modifying agent.

3.3 | Thermal properties

The crystallinity parameters, determined by DSC, i.e., melting and crystallization temperatures along with enthalpies, are presented in Table 5. Findings did not show significant modification of the melting and crystallization temperatures of the studied nanocomposites. These temperatures remained, respectively, around 140 and 113°C for PE and around 167 and 120°C for PP formulations. This observation confirms that DFNS does not present any nucleating effect. In the presence of K-STOFF, the melting and crystallization temperatures as well as corresponding enthalpies are not significantly modified. Thus, the evolution of the mechanical properties of PE and PP, obtained after the incorporation of DFNS particles and K-STOFF could not be triggered by any modification of the polymer thermal properties.

3.4 | Morphological properties

The morphology of the different nanocomposites was investigated by SEM to evaluate the dispersion state of DFNS and the quality of the filler/polymer interface (Figures 3 and 4). SEM images, presented on the left, obtained at medium magnification ($\times 10000$), show the dispersion state of nanoparticles while the images on the right, obtained at a higher magnification ($\times 80000$) focus more on the interface between the polymer matrix and particles. One can observe that the nanoparticles are well distributed and dispersed within the polymeric matrix regardless the presence or absence of K-STOFF in both PE and PP. However, most importantly, fundamental changes in the interface behavior were noted, depending both on the nature of the polymeric matrix and on the presence of the K-STOFF additive. In the case of PE containing 10 wt.% DFNS, several filaments are readily visible at the interface, highlighting an intermediate behavior between cohesive and non-adhesive interface. In fact, one can observe the presence of small, stretched polymer filaments, which remain attached to the surface of silica, and which constitute interfacial links between the two phases. To the best of our knowledge, this is the first time that such an observation has been reported for polyolefin-based nanocomposites, produced by melt compounding, containing untreated nanoparticles, and without using any compatibilizing agents. The incorporation of K-STOFF leads to important modification of the nanocomposite morphologies, and to the formation of poor interface as observed in Figure 3, which illustrates the total debonding of DFNS from the polymer matrix. It is also important to note that the pristine porosity of the DFNS is no longer observable, and a smooth surface replaces the “wrinkled” surface that was previously evidenced in the case of K-STOFF-free PE-DFNS nanocomposites. K-STOFF is most likely adsorbed to the surface of fibrous silica nanoparticles, filling their accessible pores and modifying the nature of the interactions between the polymer matrix and nanoparticles as observed for “neat” DFNS. The interface is thus transformed in such a way that polymer chains can no longer interact with the fibrous nanosilica surface covered by the K-STOFF additive. This lack of interfacial interactions is most likely the main reason behind the reduction of the mechanical properties recorded for PE nanocomposites containing the fatty amide modifying agent, particularly the transition from partial to total fracture during impact tests (Table 3).

As far as PP-based nanocomposites are concerned, DFNS remained finely dispersed in the polymer matrix even in the presence of K-STOFF (Figure 4). However, in contrast to PE-based blends, PP-DFNS nanocomposites

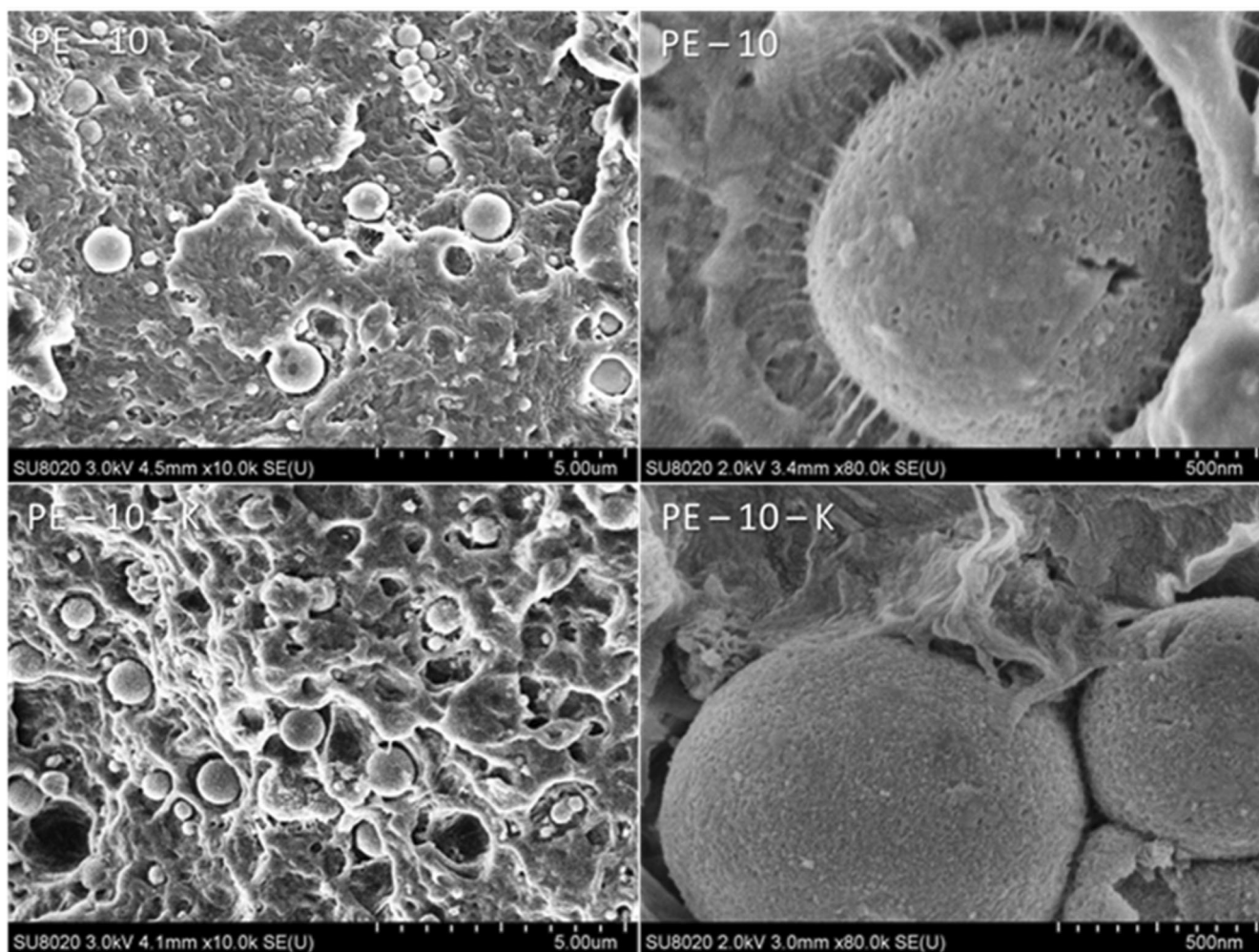


FIGURE 3 SEM images of PE nanocomposites containing 10 wt.% FSN, with (down images) and without K-Stoff (top images).

present a cohesive interface between the nanoparticles and the polymer. SEM observations evidenced that fibrous silica nanoparticles were well embedded into the PP matrix, highlighting a good affinity between both phases without any interfacial debonding. As can be observed from the images, and in the presence of K-STOFF, the wettability between the nanoparticles and the polymer chains is of lower quality, but maintains a cohesive interface without visible interfacial debonding. This limited but non-negligible alteration in the quality of the interface between the nanoparticles and PP in the presence of K-STOFF could be the origin of the decrease in the mechanical resistance of these nanocomposites during the tensile, impact, and flexion tests (Tables 3 and 4).

3.5 | Rheological behavior

Rheological analysis of polymer nanocomposites is an efficient method to assess the nanoparticle dispersion state

and the quality of the interface between fillers and a polymeric matrix. Figure 5 illustrates the complex viscosity ($\eta^*(\omega)$) at 180°C, as a function of the angular frequency of PE, PP, and related nanocomposites containing 10 wt.% DFNS with and without K-STOFF. One can observe that the incorporation of fibrous silica nanoparticles induces an increase in the viscosity at low frequency, in both PE and PP nanocomposites. This phenomenon is known as solid-like behavior and is usually attributed to particle-particle and/or particle-matrix interactions that induce polymer chain flow restrictions in the molten state.²¹ The viscosity increase is more pronounced in the case of PP nanocomposites that demonstrated high affinity with DFNS as evidenced by SEM observations (Figure 4). The alteration of the quality of the interface between silica nanoparticles and PP, highlighted through SEM observations, also explains the modification of the rheological behavior of the PP-10-K nanocomposite. Indeed, the accumulation of K-STOFF at the surface (and within the accessible pores) of the DFNS limits the interactions between the PP chains

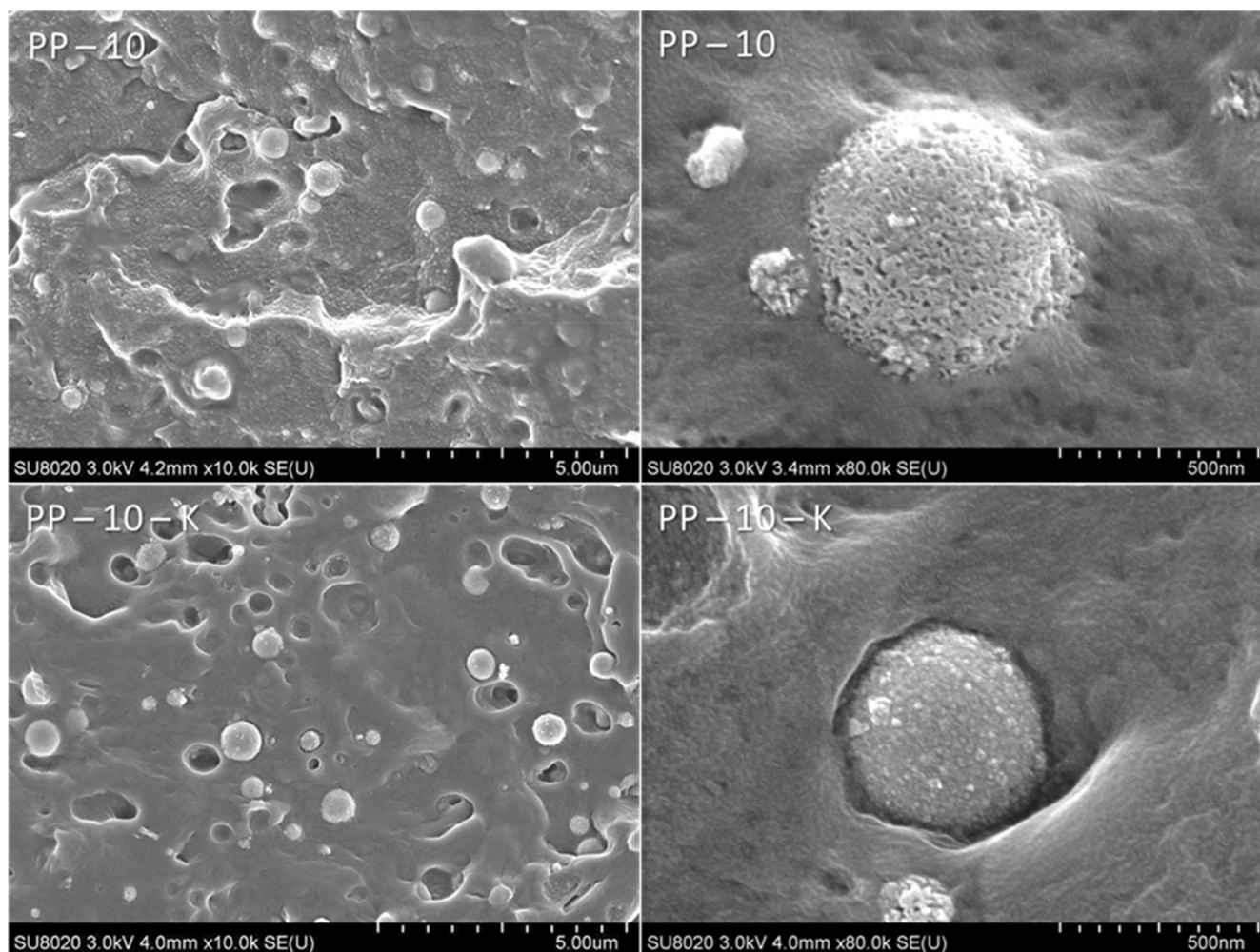


FIGURE 4 SEM images of PP nanocomposites containing 10 wt.% DFNS, with (bottom) and without (top) K-Stoff.

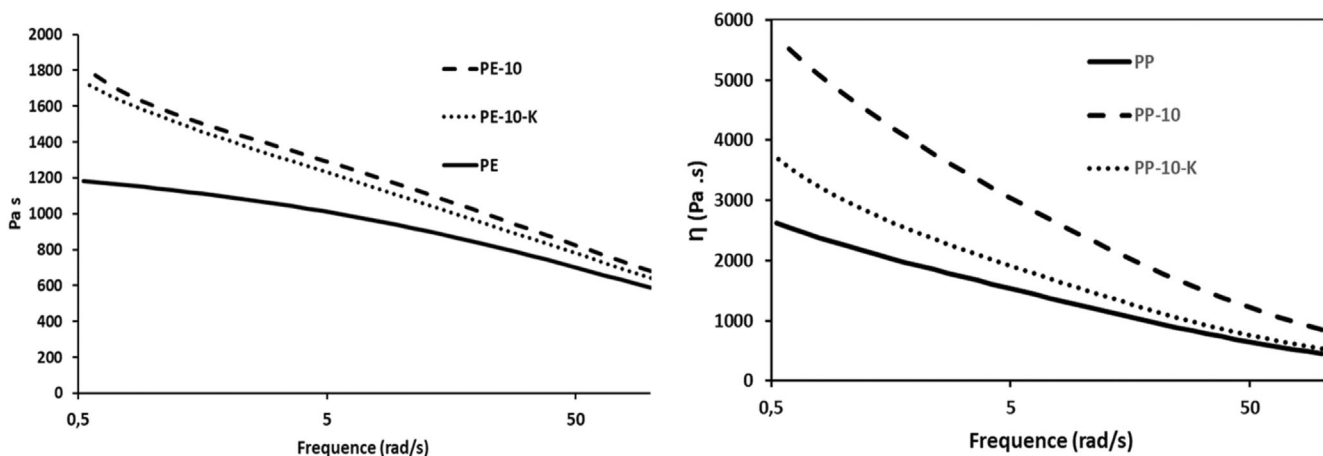


FIGURE 5 Complex viscosity of PE, PP, and 10 wt.% DFNS nanocomposites at 180°C.

and the silica particles which explains the limited increase of the viscosity of this ternary mixture. It is important to note that the viscosity of this blend (PP-10-K) remains higher than that of the pristine polymer due to the presence of DFNS, which remains well dispersed even in the

presence of K-STOFF. In the case of PE, the effect of K-STOFF on the reduction of the complex viscosity is more limited. This is likely due to the quality of the interface between PE and DFNS, which seems to be not as good as that of PP/DFNS composites, with or without

K-STOFF (Figures 3 and 4). Indeed, the presence of K-STOFF reduces the interactions between PE chains and silica, but the difference is smaller in the case of PP since the PE/DFNS interface is less cohesive than that of PP/DFNS.

4 | CONCLUSION

Well-defined DFNS particles were synthesized using a hydrothermal method and successfully incorporated as fillers with up to 10 wt.% into PE and PP matrices by twin-screw extrusion. Their morphological specificities had a significant influence on the particle/polymer interface and on the functional properties of the corresponding composites. Results showed that the interactions between the nanoparticles and polymer matrix are dependent on both the nature of the host polymer and the presence of the surface modifying agent. DFNS were well dispersed into both PE and PP, but a good interfacial wettability was obtained with PP as it has been highlighted by both SEM observations and rheological measurements. In fact, the interaction between the PP matrix and DFNS was slightly reduced in the presence of K-STOFF surface modifying agent. Owing to its good affinity with silica nanoparticles, K-STOFF accumulated at the surface and consequently reduced the interaction between the polymer matrix and nanoparticles. This effect also induced some reduction of the mechanical properties in both PP and PE-based nanocomposites. The findings of this study will open the door to further explore the benefits of the unique morphology of DFNS to develop new generation of nanocomposites with advanced functional properties.

DATA AVAILABILITY STATEMENT

The data that support the findings of this study are available on request from the corresponding author. The data are not publicly available due to privacy or ethical restrictions.

ORCID

Aziz Fihri  <https://orcid.org/0009-0000-0625-3568>

REFERENCES

- Kuila T, Tripathy T, Hee LJ. Polyolefin-based polymer nanocomposites. *Adv Polym Nanocompos*. 2012;181-215. doi:10.1533/9780857096241.2.181
- Alexandre M, Dubois P. Polymer-layered silicate nanocomposites: preparation, properties and uses of a new class of materials. *Mater Sci Eng R Rep*. 2000;28(1-2):1-63. doi:10.1016/S0927-796X(00)00012-7
- Kango S, Kalia S, Celli A, Njuguna J, Habibi Y, Kumar R. Surface modification of inorganic nanoparticles for development of organic-inorganic nanocomposites—a review. *Prog Polym Sci*. 2013;38(8):1232-1261. doi:10.1016/j.progpolymsci.2013.02.003
- Watanabe R, Hagihara H, Sato H. Structure–property relationships of polypropylene-based nanocomposites obtained by dispersing mesoporous silica into hydroxyl-functionalized polypropylene. Part 2: matrix–filler interactions and pore filling of mesoporous silica characterized by evolved gas analysis. *Polym J*. 2018;50(11):1067-1077. doi:10.1038/s41428-018-0096-9
- Bikiaris DN, Vassiliou A, Pavlidou E, Karayannidis GP. Compatibilisation effect of PP-g-MA copolymer on IPP/SiO₂ nanocomposites prepared by melt mixing. *Eur Polym J*. 2005;41(9):1965-1978. doi:10.1016/j.eurpolymj.2005.03.008
- Yuan W, Wang F, Chen Z, et al. Efficient grafting of polypropylene onto silica nanoparticles and the properties of PP/PP-g-SiO₂ nanocomposites. *Polymer*. 2018;151:242-249. doi:10.1016/j.polymer.2018.07.060
- Scharlach K, Kaminsky W. New polyolefin-nanocomposites by in situ polymerization with metallocene catalysts. *Macromol Symp*. 2008;261(1):10-17. doi:10.1002/masy.200850102
- Lin OH, Akil HM, Mohd IZ. Surface-activated nanosilica treated with Silane coupling agents/polypropylene composites: mechanical, morphological, and thermal studies. *Polym Compos*. 2011;32(10):1568-1583. doi:10.1002/pc.21190
- Russo P, Venezia V, Tescione F, et al. Improving interaction at polymer–filler Interface: the efficacy of wrinkle texture. *Nanomaterials (Basel)*. 2020;10:208-223. doi:10.3390/nano10020208
- Maiti M, Basak GC, Srivastava VK, Jasra RV. Mesoporous silica reinforced polybutadiene rubber hybrid composite. *Int J Ind Chem*. 2016;7(2):131-141. doi:10.1007/s40090-015-0062-8
- Wang N, Fang Q, Zhang J, Chen E, Zhang X. Incorporation of nano-sized mesoporous MCM-41 material used as fillers in natural rubber composite. *Mater Sci Eng A*. 2011;528:3321-3325. <https://www.sciencedirect.com/science/article/pii/S0921509311000128>
- Polshettiwar V, Cha D, Zhang XX, Basset JM. High-surface-area silica Nanospheres (KCC-1) with a fibrous morphology. *AngewChem Int Ed*. 2010;50(49):9652-9656.
- Xu C, Lei C, Wang Y, Yu C. Dendritic mesoporous nanoparticles: structure, synthesis and properties. *Angew Chem Int Ed*. 2022;61(12):e202112752. doi:10.1002/anie.202112752
- Polshettiwar V. Dendritic fibrous nanosilica: discovery, synthesis, formation mechanism, catalysis, and CO₂ capture–conversion. *Acc Chem Res*. 2022;55(10):1395-1410. doi:10.1021/acs.accounts.2c00031
- Fihri A, Abdullatif D, Saad HB, Mahfouz R, Al-Baidary H, Bouhrara M. Decorated fibrous silica epoxy coating exhibiting anti-corrosion properties. *Prog Org Coat*. 2019;127:110-116. doi:10.1016/j.porgcoat.2018.09.025
- Silver nanoparticles immobilized on fibrous nano-silica as highly efficient and recyclable heterogeneous catalyst for reduction of 4-nitrophenol and 2-nitroaniline. *Appl Catal Environ*. 2014;158-159:129-135. doi:10.1016/j.apcatb.2014.04.015
- Wang K, Liang S, Deng J, et al. The role of clay network on macromolecular chain mobility and relaxation in isotactic polypropylene/organoclay nanocomposites. *Polymer*. 2006;47(20):7131-7144. doi:10.1016/j.polymer.2006.07.067
- Hamzah MS, Mariatti M, Ismail H. Melt flow index and flammability of alumina, zinc oxide and organoclay nanoparticles filled cross-linked polyethylene nanocomposites. *Mater Today Proc*. 2019;17:798-802. doi:10.1016/j.matpr.2019.06.365
- Salmi MS, Zoukrami F, Haddaoui N. Structure-properties relation in thermoplastic polymer/silica nanocomposites in presence

- of stearic acid as modifier agent. *Int J Polym Anal Charact.* 2021; 26(7):604-617. doi:[10.1080/1023666X.2021.1947661](https://doi.org/10.1080/1023666X.2021.1947661)
20. Wetting & Dispersing Additives – Polymeric & Oleochemical Base Waxes|20 Microns Ltd. Accessed September 12, 2022. <https://www.20microns.com/wetting-dispersing-additives-polymeric-oleochemical-base-waxes/>
21. Patti A, Russo P, Acierno D, Acierno S. The effect of filler functionalization on dispersion and thermal conductivity of polypropylene/multi wall carbon nanotubes composites. *Comp Part B Eng.* 2016;94:350-359.

How to cite this article: Fihri A, Lazko J, Laoutid F, et al. Effect of interfacial modification on functional properties of polyethylene and polypropylene—Fibrous silica nanocomposites. *J Vinyl Addit Technol.* 2023;1-10. doi:[10.1002/vnl.22076](https://doi.org/10.1002/vnl.22076)